

# On the behavior of quercetin + organic solvent solutions and their role for C60 fullerene solubilization



Juan Antonio Tamayo-Ramos<sup>a</sup>, Sonia Martel<sup>a</sup>, Rocío Barros<sup>a</sup>, Alfredo Bol<sup>a,b</sup>, Mert Atilhan<sup>c</sup>, Santiago Aparicio<sup>a,d,\*</sup>

<sup>a</sup> International Research Centre in Critical Raw Materials-ICCRAM, University of Burgos, Plaza Misael Banuelos s/n, 09001 Burgos, Spain

<sup>b</sup> Department of Physics, University of Burgos, 09001 Burgos, Spain

<sup>c</sup> Department of Chemical and Paper Engineering, Western Michigan University, Kalamazoo MI 49008-5462, USA

<sup>d</sup> Department of Chemistry, University of Burgos, 09001 Burgos, Spain

## ARTICLE INFO

### Article history:

Received 10 May 2021

Revised 6 September 2021

Accepted 28 September 2021

Available online 05 October 2021

### Keywords:

Flavonoids  
Polar solvents  
Fullerenes  
Solubility  
Nanostructuring  
Molecular dynamics

## ABSTRACT

The nature of flavonoids in polar organic solvents solutions is studied using classical molecular dynamics simulations considering quercetin as an archetypical flavonoid and acetone, dimethylformamide and dimethyl sulfoxide as representatives of solvents with different polarity. The solvation, intermolecular forces (hydrogen bonding) and interactions of the flavonoid with the solvents are analyzed. Likewise, the role of quercetin on changing the solvent properties and the possibility of acting as a solubility enhancer for fullerenes (C60) are studied by considering the properties of C60 fullerene in quercetin plus polar solvents solutions. The reported results provide information on the nature of the considered complex liquid mixtures and analyze the possibility of using flavonoids as natural, non-toxic, modifiers of traditional polar organic solvents and to improve the solubility of complex solutes such as fullerene nanoparticles.

© 2021 The Authors. Published by Elsevier B.V. This is an open access article under the CC BY-NC-ND license (<http://creativecommons.org/licenses/by-nc-nd/4.0/>).

## 1. Introduction

Flavonoids constitute a group of natural compounds occurring in plants containing more than 6000 different molecules [1] with a large number of possible applications in the food and pharmaceutical industries [2,3,4]. The extraction of flavonoids from plant sources [5,6] as well as the development of commercial formulations involving these compounds, [7] considering stability [8,9], delivery [10] and bioavailability [11,12], require the use of suitable solvents. Likewise, when using flavonoids for therapeutic purposes, their solubility plays a pivotal role [13]. Moreover, physicochemical properties of flavonoids, such as their antioxidant activity [14], are solvent dependent. The complex molecular structures of flavonoids as well as the particular need of each extraction process or final product requires different types of solvents with suitable physicochemical characteristics [15,16]. Organic solvents (OSs) are typically used for flavonoids extraction and/or solubilization. Typical OSs such as acetone (ACE), methanol (META), ethanol (ETA) or acetonitrile (ACN) are considered and largely applied for

extraction, purification and stabilization of many different types of flavonoids [17,18]. Nevertheless, the microscopic roots of the flavonoids – OSs behavior, i.e. intermolecular forces, nanoscopic structuring and flavonoid solvation, have been scarcely studied. Sandoval et al. [19] studied solute – solvent interactions of different flavonoids (flavones and isoflavones) in methanol, ethanol and 2-propanol using experimental measurements and molecular dynamics simulations (MD). The role of the solvent was studied by the effect on hydrogen bonding through the available donor – acceptor sites in the flavonoid. Slimare et al. [20] studied solubility of flavonoids (quercetin, QUER; isoquercitrin; rutin) in different OSs using atomistic and mesoscale MD simulations. The reported results allowed to characterize the flavonoid – OS interactions as well as flavonoids self-aggregation. Smail et al. [21] studied flavonoid (luteolin) – OSs (alkanols, ACE, DMSO) interactions by using MD. The role of hydrogen bonding through luteolin sites plays a pivotal role in solvation and solubilization. For the case of flavonoids in mixed solvents, Jabbari et al. [22] studied the behavior of the flavonoid naringenin in aqueous dimethylsulfoxide (DMSO) mixtures using a combined experimental and computational (MD simulations) approach. The reported results probed the preferential solvation of flavonoid molecules by DMSO ones in contrast with water ones, thus leading to an increase in flavonoid solubility. Naringenin was also studied in aqueous – OSs mixtures by Tooski

\* Corresponding author at: International Research Centre in Critical Raw Materials-ICCRAM, University of Burgos, Plaza Misael Banuelos s/n, 09001 Burgos, Spain.

E-mail address: [sapar@ubu.es](mailto:sapar@ubu.es) (S. Aparicio).

et al. [23] through solubility and thermodynamics analysis, thus probing preferential solvation of the flavonoid as a function of solvent mixture content. Therefore, the available literature results show two main effects in flavonoids solubilization and solute – solvent interactions: (i) role of hydrogen bonding and (ii) preferential solvation for mixed fluids, i.e nanoscopic local heterogeneity. Nevertheless, the nanoscopic behavior of flavonoids – OSs solutions is still poorly understood. The understanding of the relationship between nanoscopic structuring and macroscopic behavior is required for the improvement of flavonoids solubilization applications as well as the development of new and suitable solvents for processing these natural compounds.

The solubilization of flavonoids in OSs leads to changes in the OSs structuring at the nanoscopic level, and thus the solvent properties regarding other solutes (non-flavonoids) should also be modified. Therefore, neat OSs solvation properties should be different to those of OSs + flavonoids solutions. This effect constitutes a way of modifying OSs by the addition of a natural compound to provide improvements regarding to the solubilization of hardly soluble compounds. A relevant technological problem in the nanomaterials processing and development industry is the low solubility in common OSs of the most relevant nanoparticles. In particular, the low solubility of fullerenes [24,25], because of their high hydrophobic character, in the most common OSs hinders the development of suitable and stable fullerene – OS dispersions to be applied for the considered technologies [26]. Fullerenes are poorly soluble in the vast majority of polar OSs [27,28], which results in the need of using low polar OSs, mainly aromatics such as benzene, toluene or derived compounds, which leads to remarkable environmental and toxicological problems [29]. Molecular level insights have been inferred on the factors improving fullerenes solubility in OSs [30], which may be used for the design of new solvents for fullerenes solubilization [31] as well as for the improvement of solubility in polar OSs. A possible approach considered in this work stands on the modification of the OSs properties by the addition of flavonoids, and as a consequence, the improvement of fullerenes solubility in OSs. The research reported in this work considers an archetypical flavonoid, quercetin (QUER), belonging to the flavonol type of flavonoids. The behavior of this flavonoid in three selected OSs (acetone, ACE; N,N-dimethylformamide, DMF; dimethyl sulfoxide, DMSO) was studied. Although recent studies have proposed the use of neoteric green solvents for the extraction of flavonoids [32], most of the available processes consider OSs as extractant or solubilizing agents, thus the knowledge of flavonoids – OSs solutions is of pivotal interest. Likewise, the properties of fullerene C60 in QUER – ACE, QUER-DMF and QUER-DMSO solutions was studied, Fig. 1. The experimental solubilities of QUER in the considered OSs as well as for C60 in the same OSs are reported in Table 1 [24,33] probing moderately (QUER) to low (C60) solubility in both cases. The three selected OSs (ACE, DMF and DMSO) are polar solvents but with polarity increasing on going from ACE ( $\mu = 2.69$  D) to DMF ( $\mu = 3.86$  D) to DMSO ( $\mu = 4.1$  D). Therefore, the effect of solvent polarity on QUER and C60 solubility may be inferred with the three considered polar OSs.

The properties of the considered complex solutions (QUER in OS and C60 in QUER + OS) were studied considering classical molecular dynamics simulations (MD). MD simulations have been previously considered in the literature to provide suitable characterization of flavonoids – OSs [20,22,34] solutions as well as for the study of fullerenes – OSs solutions [31,35,36,37,38].

The use of MD simulations allows to infer the nature of specific interactions of solute with solvents, such as intermolecular forces or solvation mechanisms, which can not be captured with other theoretical approaches such as the use of quantum chemistry methods using continuum models to describe solvent effects [39]. This theoretical approach provides a detailed characterization

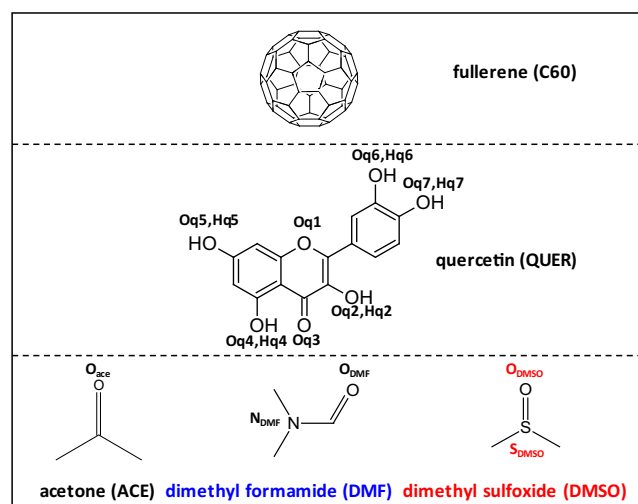


Fig. 1. Molecular structures of compounds used in this work. Atom Labelling used along this work is indicated.

**Table 1**  
Experimental solubility ( $x$ , mole fraction) of QUER and C60 in OSs.

	log( $x$ )	T/K	Reference
<b>QUER in OSs</b>			
ACE	-2.23	323	[33]
DMF	-	-	-
DMSO	-	-	-
<b>C60 in OSs</b>			
ACE	-7	298	[24]
DMF	-5.3	298	[24]
DMSO	-	-	-

of the nanoscopic behavior of the considered systems in terms of structuring, solvation and intermolecular forces, thus providing queues on the solubility of both flavonoids and fullerenes in the considered OSs. Therefore, the reported study has two main objectives: (i) characterize flavonoids (QUER) – OSs solutions and (ii) analyze the behavior of fullerenes (C60) in flavonoid – OSs solutions, to explore the possible improvement of fullerenes solubility in OSs by using flavonoids as solubility enhancers.

## 2. Methods

MD simulations for were carried out using MDynaMix v.5.2 [40]. The considered simulation boxes are reported in Table S1 (Supplementary information), the simulated concentrations for QUER in OSs are in the same range as those experimental as reported in Table 1, whereas for C60 the MD studied solutions (Table S1, Supplementary Information) are more concentrated than the experimental data (Table 1) for computational reasons to maintain the simulation boxes in a reasonable size, although they are diluted enough to resemble the behaviour of C60 in the studied OSs in presence of QUER. The simulated solutions correspond to roughly  $5 \text{ mg mL}^{-1}$  C60 content, whereas experimental solubilities are roughly 0.05 (DMF) to 1 (DMSO)  $\text{mg mL}^{-1}$  C60. Nevertheless, the considered MD box sizes hinders the interaction between neighbour C60 molecules, thus being representative of highly diluted C60 solutions.

The initial cubic simulation boxes were built using Packmol [41] program. To avoid any effect derived from the characteristics of the initial configuration in the final results, 10 different initial configurations for each of the compositions reported in Table S1 (Supplementary Information) were built with Packmol [41], considering densities in the  $0.95 \rho_{OS}$  to  $1.05 \rho_{OS}$  (where  $\rho_{OS}$  stands for the den-

sity of each OS at 303 K). The analysis reported along this work considers the average of the properties of the 10 trajectories for each mixture.

The force fields applied for the involved molecules is reported in Table S2 (Supplementary Information). The Force field parameters for OS molecules were obtained from SwissParam database (Merck Molecular Force Field [42]) as reported in Table S2 (Supplementary Information). C60 fullerene was considered as composed of uncharged  $sp^2$  carbon atoms interaction via Lennard-Jones potential, with the C60 molecule treated as a non-rigid entity with the internal force field parameters as reported in Table S2 (Supplementary Information). MD simulations were carried out in a two steps procedure in order to obtain both velocity distributions and density profiles accurately: *i*) initial simulation boxes were subjected to NVT simulations at 303 K for 10 ns and *ii*) followed by NPT simulations at 303 K and 1 bar for 100 ns. The equilibration was assured by analysing the system potential energy and relevant physicochemical properties such as density as a function of simulation time. The control of systems temperature and pressure was done using the Nose-Hoover method, with 0.1 and 0.5 ps coupling times for temperature and pressure, respectively. The equations of motion were treated with the Tuckerman-Berne double time step algorithm [43], with 1 and 0.1 fs for long- and short-time steps. The Ewald method [44] (15 Å for cut-off radius) was used for treating electrostatic interactions. The Lennard-Jones potential was considered, with 15 Å cut-off and Lorentz-Berthelot mixing rules for calculating cross interaction terms. The analysis and visualization of MD results was carried out with TRAVIS [45] and VMD [46] programs.

Finally, although available literature reports toxicity of C60 fullerene [47], the ecotoxicological properties of the studied mixtures are considered in this work by an *in silico* approach using ADMET-STAR 2.0 software tool [48]. The machine learning methods implemented in ADMETSTAR 2.0 allows the prediction of relevant ecotoxicological properties of chemicals from the available databases. SMILES for the molecules were created for the structures of each system (neat C60, C60 + OS and C60 + OS + QUER) and used as input files for the ecotoxicological predictions.

### 3. Results and discussion

#### 3.1. Quercetin in organic solvents

The flavonoid QUER is moderately soluble in the considered OS, e.g. literature experimental results reported in Table 1 show  $\log(x)$ , where  $x$  stands for QUER mole fraction, being  $-2.23$  at 323 K, which corresponds to 24 g QUER  $\text{mL}^{-1}$  ACE. Thus, the simulated systems corresponding to these diluted solutions although may lead to QUER – QUER self-association, the main features controlling the behavior of QUER – OSs should come from QUER – OSs heteroassociations. QUER molecule may act as *i*) hydrogen bond donor, through oxygen sites (Oq2,4,5,6,7), and *ii*) hydrogen bond acceptor (through oxygen sites Oq1 to Oq7), Fig. 1. Therefore, QUER molecule is prone to develop extensive hydrogen bonding both through homo and heteroassociation. The considered polar OSs (ACE, DMF and DMSO) may act only as hydrogen bond acceptors through the corresponding CO or SO sites. The neat OSs are self-associated mainly through dipolar interactions [49,50], although weak self-hydrogen bonding is proposed in the case of DMF [51]. Therefore, the solubilization of QUER in the studied OSs should lead to a competition between the QUER – OS heteroassociation through hydrogen bonding and the disruption of OS – OS self-association by dipolar interactions, i.e. the QUER solute should disrupt the dipolar aggregation of rh solvents for the development of the stronger heteroassociations by hydrogen bonding. The nature

of the developed intermolecular forces in QUER – OS mixtures is firstly analyzed from MD simulations considering the intermolecular interaction energy,  $E_{inter}$ , as reported in Fig. 2 for all the possible interacting pairs. The  $E_{inter}$  is defined as the sum of coulombic and Lennard-Jones intermolecular contributions in the simulation boxes for each molecular pair.

The  $E_{inter}$  shows two main results for the three considered polar OSs: *i*) QUER molecules are not self-associated in the studied solutions as inferred from the close to zero  $E_{inter}$  values reported for QUER – QUER interactions, and *ii*) QUER is largely hydrogen bonded with the OS, as the large  $E_{inter}$  values for QUER – OS pairs indicate. Likewise, the strength of QUER – OS interactions follows the ordering ACE < DMF < DMSO, which can be justified considering the increasing polarity from ACE to DMF to DMSO. Moreover, OS – OS interactions are an order of magnitude weaker than QUER – OS ones, which indicates dipolar interactions for the OS – OS self-association in contrast with QUER – OS heteroassociations through hydrogen bonding.

The properties of the solutions are further analyzed considering relevant site – site radial distribution functions (RDFs), Fig. 3. The reported RDFs show QUER – OS interactions developing hydrogen bonding through the QUER donor sites (OH groups Oq2,4,5,6,7, Figs. 1 and 3) whereas the interactions through QUER acceptor sites (Oq1,3) are not hydrogen bonds (Fig. 3a and c). The interaction through all the OH sites in QUER shows the same characteristics with a narrow and intense first RDF peak with maxima at 2.8–2.9 Å corresponding to a hydrogen bond. The interaction through the Oq4 OH site, Fig. 3d, shows a first RDF peak with maxima at longer distances (3.2 Å) and being weaker and wider, which corresponds to a weaker interaction through this site. This weaker interaction through the Oq4 site may be produced by steric hindrance to interact through this site in comparison with the remaining available OH sites in QUER molecule. Additional features in RDFs are inferred up to roughly 10 Å, which show the development of solvation arrangements around QUER molecules beyond the first solvation shell around the flavonoid. The effect of the type of OS on the considered RDFs is very minor, with peaks maintaining their position and shape, with only certain changes in the peak intensity, thus the polar OS only (minimally) changes the extension of hydrogen bonding but not the interaction mechanisms.

Further analysis of the QUER – OS interactions is carried out through the so-called connection matrix analysis (*cmat*) [52], Fig. 4 and Figure S1 (Supplementary Information). For *cmat* analysis atomic pairs are considered, those atoms which may develop hydrogen bonding are considered and all the possible hydrogen bond donor and hydrogen bond acceptor atoms are considered as pairs. For these atomic pairs RDFs are calculated, the height and distance of the first RDF peak are calculated (which correspond

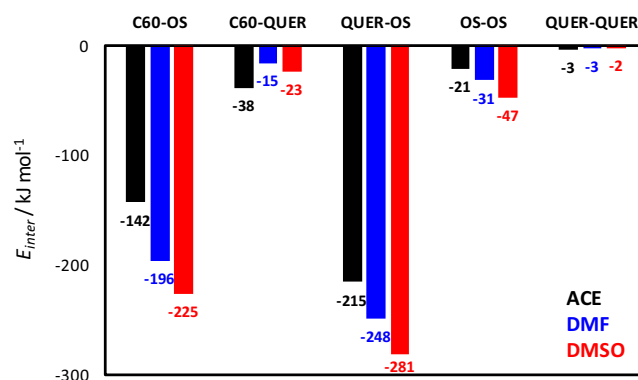
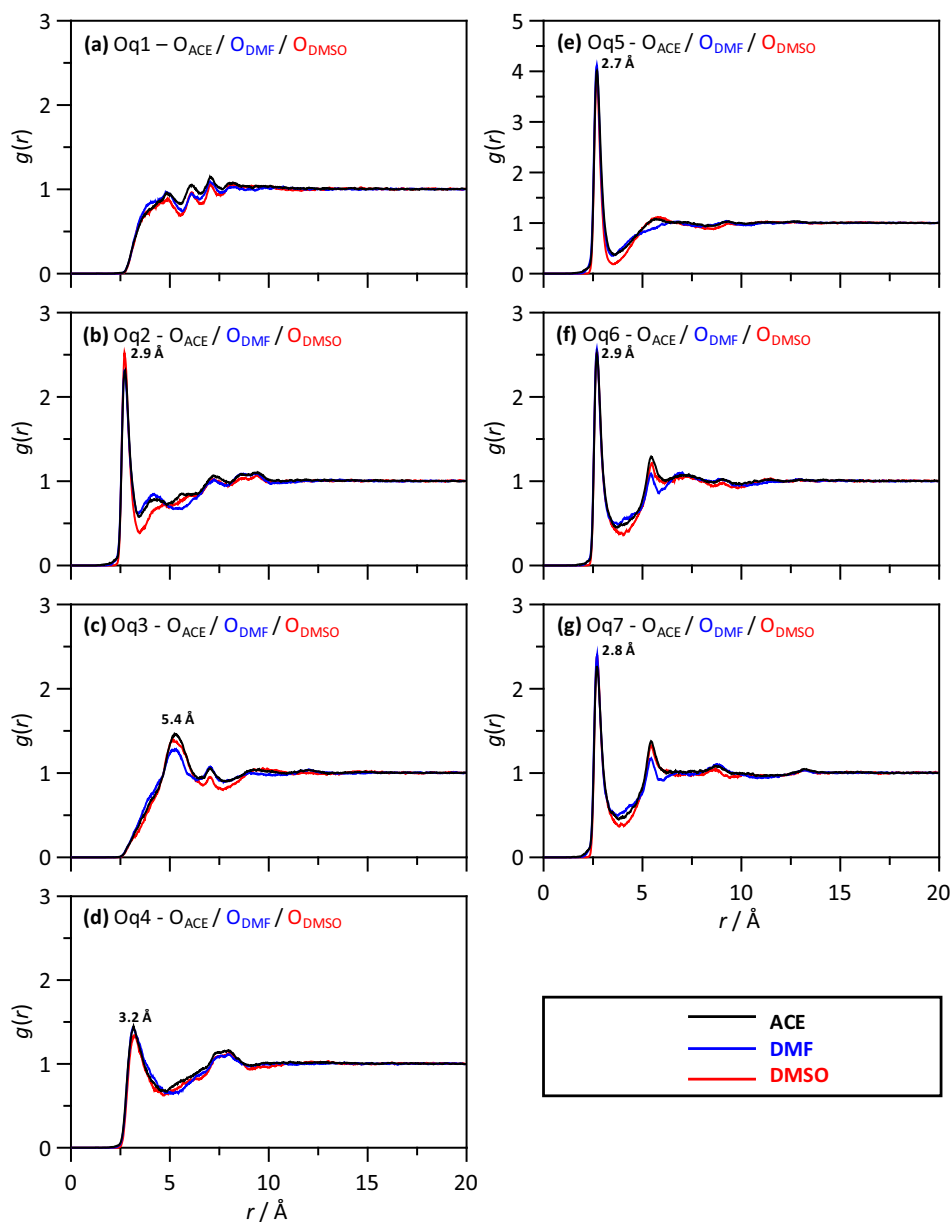


Fig. 2. Intermolecular interaction energy,  $E_{inter}$ , for the reported pairs in C60 + QUER + OS (OS = ACE, DMF or DMSO) solutions at 303 K and 1 bar.



**Fig. 3.** Site-site radial distribution functions,  $g(r)$ , for the reported atomic pairs (atom labelling as in Fig. 1) showing QUER – OS interactions in C60 + QUER + OS (OS = ACE, DMF or DMSO) solutions at 303 K and 1 bar.

to hydrogen bond interaction) and they are plotted in a color scheme which is used to indicate the strength of hydrogen bonding. Therefore, short interatomic distances and large peak intensities inferred from RDFs and plotted in *cmat* analysis would indicate strong hydrogen bonding. Results in Fig. 4 and Figure S1 (Supplementary Information) report *cmat* analysis for the considered solvents and possible QUER – QUER and QUER – OS interactions. The *cmat* for QUER – QUER interactions discards QUER homoassociations by hydrogen bonding. The color scheme indicates the strength of the interactions, e.g. red color indicating short distance and large RDF peak indicates the stronger hydrogen bonding. For QUER – OS interactions, *cmat* analysis, indicates hydrogen bonding through Hq2,4,5,6,7 sites for all the considered OS with weaker interactions (yellow code) for Hq4 site, as previously indicated in Fig. 3. The effect of the type of solvent is minor, mainly DMSO leads to weaker interactions for all the considered sites, Fig. 4c. This is in contrast with the larger  $E_{inter}$  values for QUER – DMSO in compar-

ison with ACE and DMF, which may be justified considering that the increase of OS polarity on going to DMSO leads to a certain rearrangement around the QUER molecules to favor dipolar interactions, thus slightly changing the hydrogen bonding interactions. Nevertheless, these changes are minor and QUER is hydrogen bonded to all the considered polar OSs, Fig. 3.

The reported RDFs provide the distribution around QUER molecules as a function of distance, i.e. the position of solvation shells, but not the exact spatial arrangement of OS molecules around the central QUER, which can be inferred from the Spatial Distribution Functions (SDFs) reported in Fig. 5. SDFs for all the considered OSs show analogous distribution around the OH sites in QUER, with OS molecules being placed around all the QUER OH sites with the exception of Oq4 site, which is free of QUER molecules probably because of steric hindrance. The SDF cap above the Oq1 site (ether site) show also OS molecules concentrating around that site are although without forming hydrogen bonding because the cap is

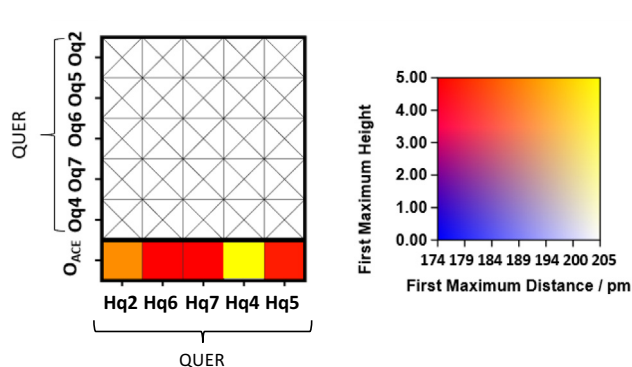


**Fig. 4.** Connection matrix analysis for possible hydrogen bonds in C60 + QUER + ACE solutions at 303 K and 1 bar. Rows represent hydrogen bond acceptor sites (oxygen atoms) and columns represent hydrogen atoms in hydrogen bond donor sites. Atom labelling as in Fig. 1. The color of each square corresponds to the intensity and distance of the first maximum in the corresponding radial distribution functions with the color scale indicated in the panels on the right.

placed at longer distances than those caps around the QUER OH sites. Therefore, a largely localized distribution of OS molecules around the OH groups of QUER is inferred for all the OSs. The distribution of molecules around QUER molecules may be also analyzed through the molecular surface coverage as reported in Fig. 6, which confirms that QUER surface is covered mostly (greater than 96 %, Fig. 6b) by OS molecules. Likewise, OS molecules (Fig. 6c) are surface covered by surrounding OS molecules, which agrees with the low content of QUER in the studied solutions. Almost negligible changes are inferred considering the type of OS in agreement with SDFs reported in Fig. 5.

The extension of QUER – OS hydrogen bonding was quantitatively determined considering a geometrical criterion (3.5 Å and 60° for donor – acceptor separation as limit values) and values per QUER molecule are reported in Fig. 7. The hydrogen bonding through Oq2,5,6 and 7 sites is confirmed, with roughly 0.5 hydrogen bonds per site for Oq2,6 and 7 sites, and 0.8 for Oq5, which seem to be the preferred interaction site as confirmed by the large cap around that site in SDFs reported in Fig. 5. Negligible interaction through Oq4 is confirmed again. Likewise, a slight increase in the number of hydrogen bonds on each site is inferred on going from ACE < DMF < DMSO, in agreement with the increase in  $E_{inter}$  reported in Fig. 2. Thus,  $cmat$  results in Fig. 4 indicate not a decrease of the QUER – OS hydrogen bonding, as discarded from results in Fig. 6, but a slight change in arrangements of the interaction. The total number of hydrogen bonds per QUER molecule is in the 2.3 to 2.7 range, increasing with ACE < DMF < DMSO, thus confirming the large extension of heteroassociation. The formation of hydrogen bonding considering the geometrical distance – angle criteria is confirmed through the reported Combined Distribution

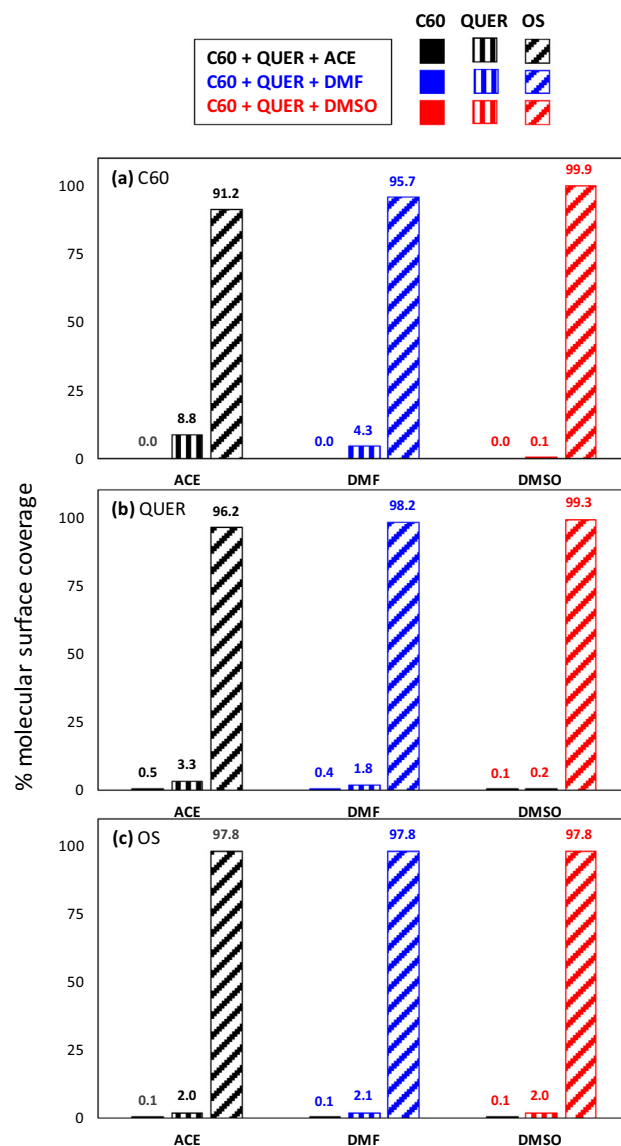


**Fig. 6.** Surface coverage of (a) C60, (b) QUER and (c) OS (ACE, DMF or DMSO) molecules in C60 + QUER + OS (OS = ACE, DMF or DMSO) solutions at 303 K and 1 bar. Very small values are obtained for C60 (solid colors, bars close to the axis).

Functions (CDFs) reported in Fig. 8. The CDFs spots at donor – acceptor distances ( $\sim 1.9$  Å) and angles ( $\sim 175^\circ$ ) show the most efficient donor – acceptor orientations leading to QUER – OS hydrogen bonding.

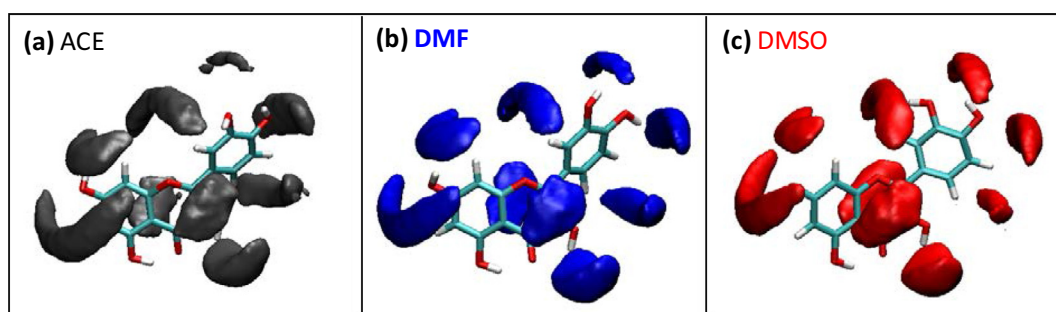


**Fig. 5.** Spatial distribution functions around QUER molecule showing the arrangement of OS molecules in C60 + QUER + OS (OS = ACE, DMF or DMSO) solutions at 303 K and 1 bar.

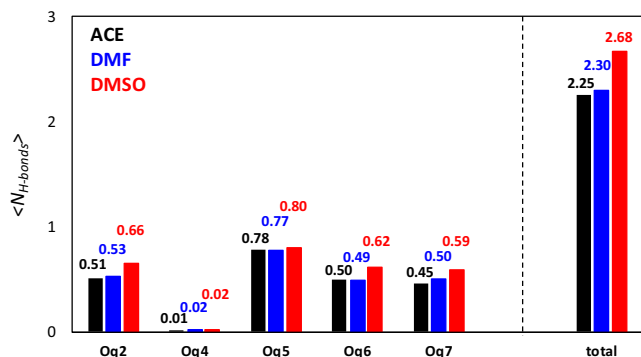


**Fig. 7.** Average number of hydrogen bonds per QUER molecule,  $\langle N_{H-bonds} \rangle$ , for QUER – OS interactions, considering the reported oxygen atoms in hydroxyl groups of QUER as donors and the oxygen atoms in OS as acceptors in C60 + QUER + OS (OS = ACE, DMF or DMSO) solutions at 303 K and 1 bar. Criteria for hydrogen bond definition: 3.5 Å and 60° for donor – acceptor separation and angle, respectively.

The dynamics of the QUER – OS hydrogen bonding is analyzed through the reactive flux analysis method [52], which allows to calculate the lifetime of a formed hydrogen bond ( $\tau_f$ ) as well as the timespan for a broken hydrogen bond to be reformed ( $\tau_b$ ), Fig. 9. A largely dynamic picture of QUER – OS hydrogen bonding is inferred for all the QUER interacting sites with  $\tau_f$  in the 5 to 32 ps range and  $\tau_b$  ( $\tau_b < \tau_f$ ) in the 4 to 37 ps. The reforming of a broken hydrogen bond takes short times, which show the large affinity of OS molecules for the QUER OH sites. Nevertheless, the reported results show QUER – OS forming and reforming in a few ps timespan, and although lifetimes of the formed hydrogen bonds follow ACE < DMF < DMSO, a very dynamic hydrogen bonding network is inferred. Likewise, self-diffusion coefficients,  $D$ , were calculated for the considered solutions using calculated mean square displacements,  $msd$ , and Einstein’s equation, Fig. 10. The low viscosity of the considered solutions, the low QUER concentration does not change remarkably the neat solvents viscosity, and the considered MD simulation time (100 ns) lead to fully diffusive regimes, which is assured through the calculation of the slopes ( $\beta$ ) of log–log plots of  $msd$  vs simulation time, leading to  $\beta$  values in the 0.98 to 1.00 range. Although  $D$  values for QUER are slightly lower than the corresponding OS, the diffusion of QUER molecules is largely coupled to that for the OS molecules (moving only slightly faster), which is produced by the large QUER – OS hydrogen bonding. Likewise,  $D$  (QUER) decreases following ACE < DMF < DMSO, which is produced because the increase of OS viscosity in ACE (0.2966 mPa s at 303.15 K [53]) < DMF (0.754 mPa s at 303.15 K [54]) < DMSO

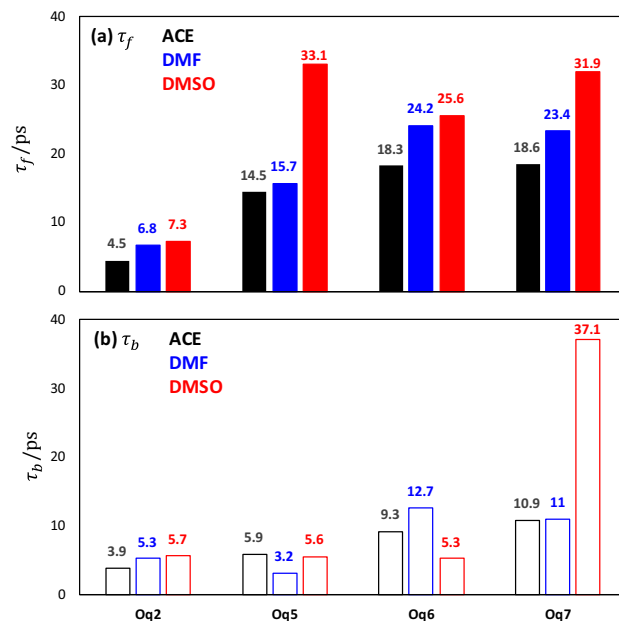


**Fig. 9.** Reactive flux analysis of the hydrogen bonding between the indicated oxygen atoms in QUER (atom labelling as in Fig. 1) and the oxygen atoms in OS, with the reported oxygen atoms in hydroxyl groups of QUER as donors and the oxygen atoms in OS as acceptors in C60 + QUER + OS (OS = ACE, DMF or DMSO) solutions at 303 K and 1 bar. Hydrogen bonding criteria as in Fig. 5.

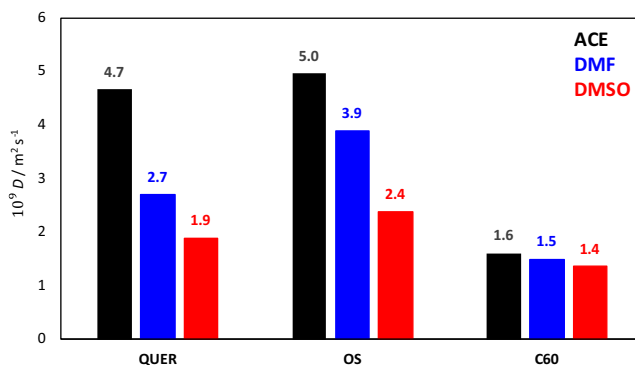


**Fig. 10.** Center-of-mass self-diffusion coefficient,  $D$ , for the reported molecules in C60 + QUER + OS (OS = ACE, DMF or DMSO) solutions at 303 K and 1 bar.

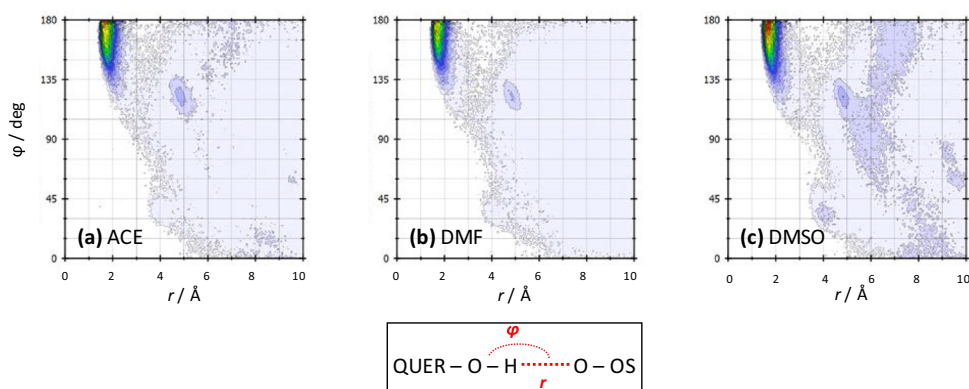


**Fig. 8.** Combined distribution functions for the reported distance,  $r$ , and angle,  $\phi$ , for the interaction between the hydroxyl oxygen atoms in QUER (Oq5–Hq5, atom labelling as in Fig. 1) and the oxygen atoms in OS, in C60 + QUER + OS (OS = ACE, DMF or DMSO) solutions at 303 K and 1 bar.

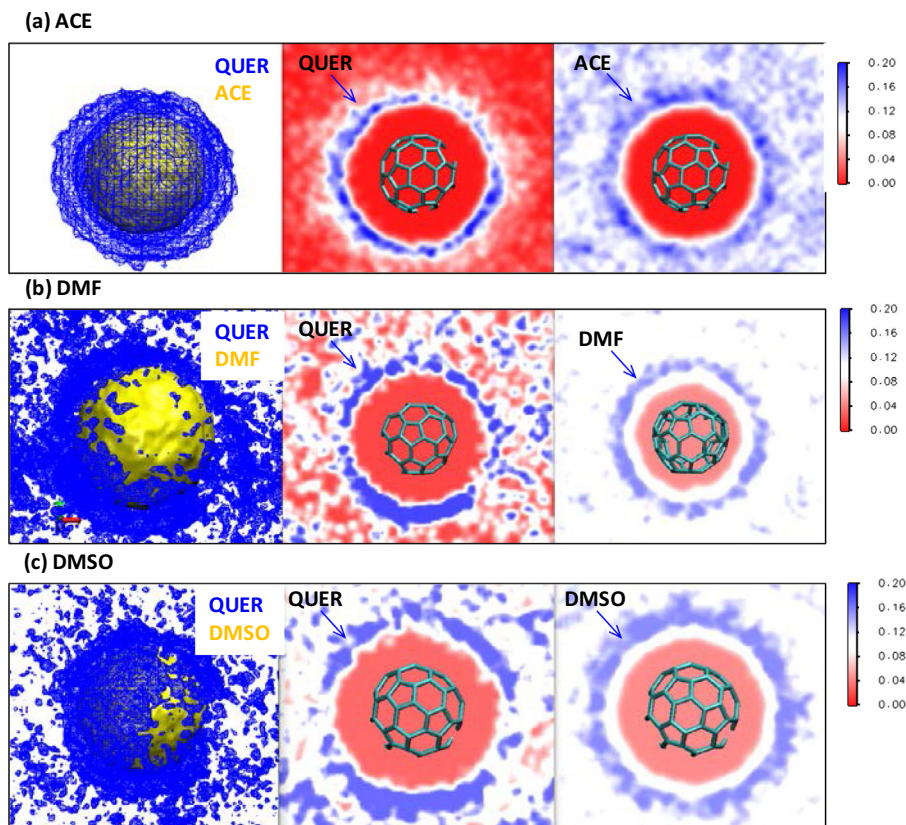


**Fig. 11.** Distribution of QUER and OS molecules around a central C60 molecule in C60 + QUER + OS (OS = ACE, DMF or DMSO) solutions at 303 K and 1 bar. The first column shows isosurfaces for QUER and OS in the first solvation shell around the central C60; the second and third column show slices along the C60 center-of-mass for QUER (second column) and OS (third column).

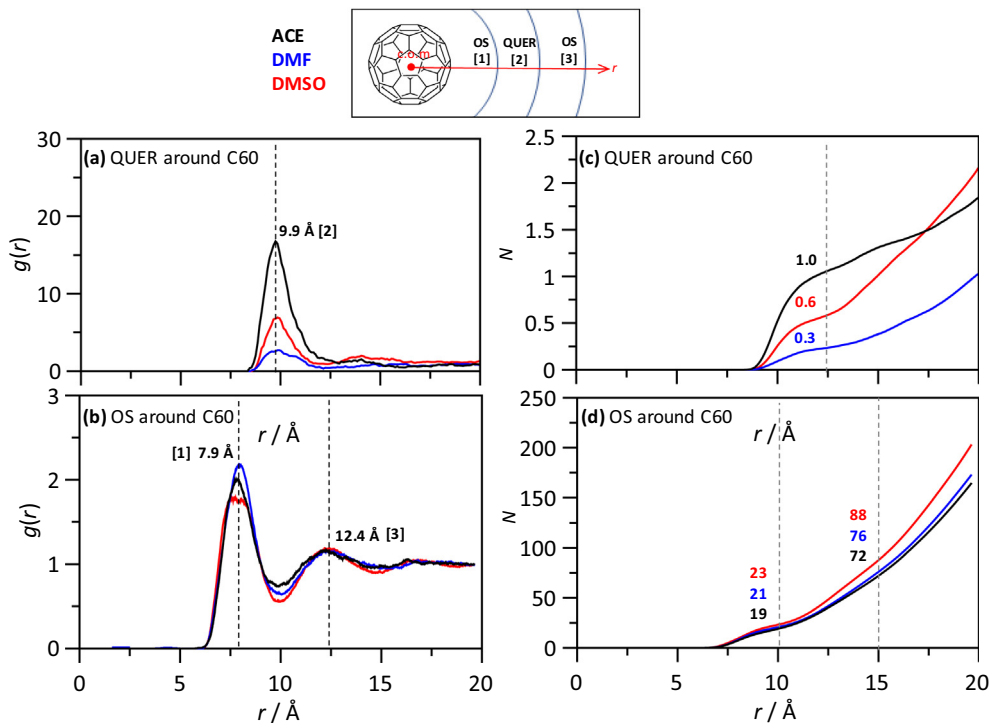


**Fig. 12.** Radial distribution functions,  $g(r)$ , between the center-of-mass (c.o.m.) of C60 and the c.o.m. of (a) QUER or (b) OS in C60 + QUER + OS (OS = ACE, DMF or DMSO) solutions at 303 K and 1 bar. Results in panels (c) and (d) show the solvation numbers,  $N$ , obtained from the integration of  $g(r)$ . Dashed lines in panels (a,b) show the position of the first maxima in  $g(r)$ . Dashed lines in panels (c,d) show  $N$  in the first solvation shell around C60 defined as the position of the first minima in  $g(r)$  in (a,b). The scheme on top of the figure shows the distribution of molecules around a central C60.

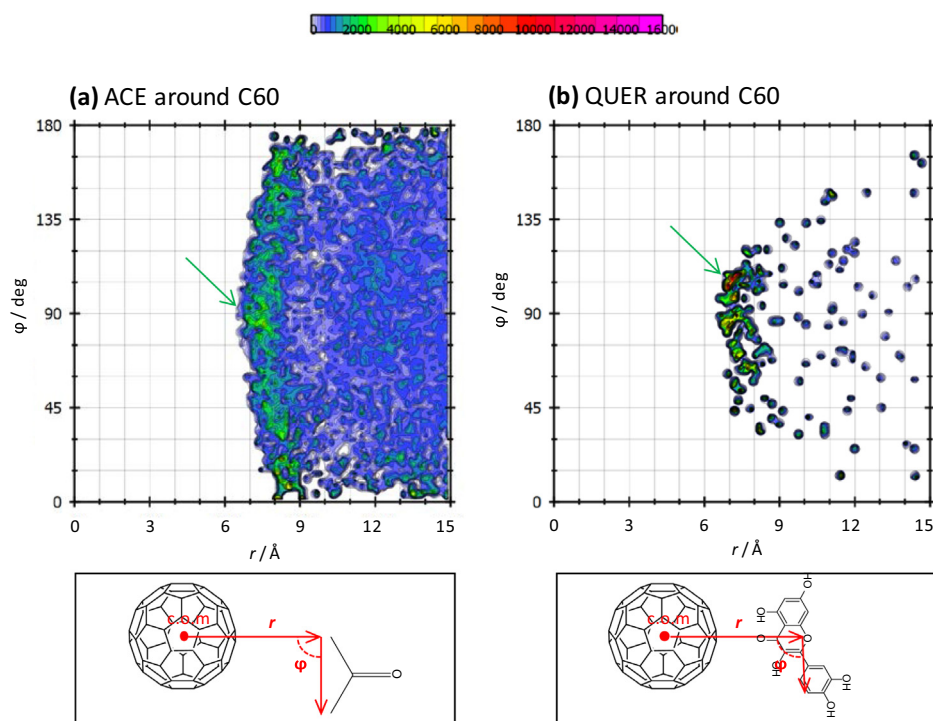


**Fig. 13.** Combined distribution functions for the reported distances,  $r$ , and angles,  $\phi$ , for the arrangement of (a) ACE and (b) QUER molecules around a central C60 molecule, in C60 + QUER + ACE solutions at 303 K and 1 bar.

(1.788 mPa s at 303.15 K [54]), i.e. decrease in  $D$ , as well as for the strengthening of QUER - OS interactions in the same ordering (Figs. 2 and 7).

### 3.2. C60 fullerene in organic solvents with quercetin

The results reported in the previous section showed polar OS rearrangement around the QUER molecules to develop heteroassociation through hydrogen bonding, thus restructuring of the considered flavonoid presence. In this section we analyze the solvation of C60 fullerene in QUER - OS solutions to infer the effect of the considered flavonoid on the behavior of the fullerene in the studied polar solutions. The strength of interactions involving C60 fullerene are quantified through  $E_{inter}$  as reported in Fig. 2. The  $E_{inter}$  values are larger for C60 - OS than for C60 - QUER pairs, which points to a preferential solvation by OS molecules (following ACE < DMF < DMSO) in spite of their polar character. This effect is confirmed by the percentage of C60 surface coverage, Fig. 6, which show how C60 surface is covered by OS molecules, with the percentage increasing with OS polarity, with negligible QUER coverage for DMSO on the C60 surface. The distribution of molecules around C60 is analyzed by the SDFs reported in Fig. 11 (where blue regions indicate high density of solvents around the nanoparticle). For all the considered polar OSs, a first solvation shell around the C60 corresponding to OS molecules in direct contact, solvation, of C60 is inferred (yellow surface) with a second solvation shell on top of it corresponding to QUER molecules. Therefore, solvation of C60 is highly heterogeneous with a OS region encasing the fullerene and it also encased by a external QUER shell. The main difference in the nature of the solvation shells with the considered OS stands on the more diffuse character of solvation shells with increasing solvent polarity as it may be inferred from comparing the results for DMSO with ACE. A more quantitative description of the solvation shells may be inferred from the RDFs reported in Fig. 12 showing the center-of-mass RDFs

for C60 and OS / QUER molecules. These RDFs confirm the OS - QUER - OS solvation shells around the central C60 molecule for the three considered OSs. The increasing polarity decreases the QUER RDF peak intensity, as inferred from the diffuse layers in Fig. 11 which leads to a decrease in the number of QUER molecules in the QUER solvation shell as inferred from Fig. 12, but maintains the solvation structuring. Previous literature results for DMSO - water [55] also showed an enrichment of the first solvation shell with DMSO polar molecules although in that case water molecules were also present, although in minor concentration, in the first shell. Nevertheless, results in Figs. 11 and 12 show a total exclusion of QUER molecules in the first shell, with flavonoid molecules being exclusively placed in the second shell around C60. Previous works in our group have shown a trend of species that build up two-dimensional materials, as carbon, to introduce a short range layer order in liquids [56,57,58]. This sandwiched structure of QUER molecules between two OS shells for solvating the C60 leads to an additional stabilization of the C60 in the solution, Fig. 2, by improving the fullerene - OS and fullerene - QUER (weaker) interactions as well as the QUER - OS interactions (hydrogen bonding) are maintained, which would also improve the separation related processing. The larger size of QUER molecules compared with those for OSs also leads to steric hindrance for placing these flavonoid molecules in the first solvation shells around the fullerene, and thus, a larger number of QUER molecules may be surrounding the C60 when QUER stand on the second solvation shell. The CDFs reported in Fig. 13 showing the orientation of OS and QUER molecules in the shells around the C60 show a slight trend of both molecules to be placed in parallel to the fullerene surface (green arrows in Fig. 13), but this trend is not so remarkable and then other orientations are also possible.

The dynamic properties of C60 in the studied mixed systems are analyzed considering the  $D$  values reported in Fig. 10. These results show slower diffusion rates for C60 than for QUER and OS molecules, which may be justified considering the bulkier size of C60,

**Table 2**

*In silico* predicted ecotoxicological properties for the systems studied in this work. (–) indicates non toxic, (+) indicates toxic, (III) for acute oral toxicity indicates slightly toxic, {} values indicate the probability for each property. Results in bold indicate toxicity for the reported property.

property	C60	C60 + ACE	C60 + DMF	C60 + DMSO	C60 + ACE + QUER	C60 + DMF + QUER	C60 + DMSO + QUER
carcinogenicity	(–) {0.5879}	(–) {0.5879}	(–) {0.7022}	(–) {0.6022}	(–) {0.9857}	(–) {0.9714}	(–) {0.9714}
eye irritation	<b>(+) {0.9819}</b>	<b>(+) {0.9905}</b>	<b>(+) {0.9781}</b>	<b>(+) {0.9806}</b>	<b>(+) {0.9473}</b>	<b>(+) {0.9264}</b>	<b>(+) {0.9291}</b>
ames mutagenesis	(–) {0.6300}	(–) {0.5600}	(–) {0.6600}	(–) {0.5300}	<b>(+) {0.8200}</b>	<b>(+) {0.7400}</b>	<b>(+) {0.8300}</b>
biodegradation	(–) {0.7000}	<b>(+) {0.5250}</b>	(–) {0.7500}	(–) {0.5750}	(–) {0.8250}	(–) {0.8500}	(–) {0.8500}
crustacea aquatic toxicity	<b>(+) {0.7800}</b>	(–) {0.8300}	<b>(+) {0.5600}</b>	<b>(+) {0.5900}</b>	(–) {0.6000}	(–) {0.5500}	(–) {0.5100}
fish aquatic toxicity	<b>(+) {0.9774}</b>	<b>(+) {0.9522}</b>	<b>(+) {0.8495}</b>	<b>(+) {0.9534}</b>	<b>(+) {0.9694}</b>	<b>(+) {0.8595}</b>	<b>(+) {0.9611}</b>
acute oral toxicity	(III) {0.7908}	(III) {0.7447}	(III) {0.6502}	(III) {0.5090}	(III) {0.6034}	(III) {0.6023}	(III) {0.5745}
water solubility (logS)	–6.735	–4.853	–3.323	–3.832	–3.302	–2.642	–3.048

the large  $E_{inter}$  values for C60 molecules (Fig. 2) as well as for the layered solvation shells around the fullerene hindering C60 mobility.

The reported results for C60 solvation in the QUER – OS solutions shows a very efficient fullerene solvation through a layered structuring around C60 favored by strong QUER – OS interactions, which points to QUER (and probably other flavonoids) as natural enhancers of fullerenes solubility in polar solvents.

### 3.3. Toxicity and ecotoxicity prediction

The selected relevant properties of the studied systems were predicted and reported in Table 1. Literature studies on C60 fullerene toxicity showed how pristine C60 leads to moderate toxicity [59]; nevertheless, *in silico* prediction of certain relevant ecotoxicity indicators was also calculated in this work, Table 2. The main problem for pristine C60 from the environmental effect would stand on their effect on aquatic living things, although this effect is of limited relevance considering the low water solubility. The preparation of C60 – OS solutions does not lead to large changes in ecotoxicity problems beyond the increase in water solubility, which will lead to larger effects on aquatic organisms. In the case of C60 + OS + QUER solutions, the addition of QUER as solvent enhancer has a main effect the increase of mutagenesis ability of the mixed fluid in comparison with the neat nanomaterial but at the same time a decrease of the carcinogenicity. Likewise, the addition of QUER increase the biodegradation ability. Therefore, the solubilization of C60 with QUER as enhancer leads to more biodegradable materials with additional properties similar to those of neat fullerenes, and thus, the OS + QUER solvents are a suitable option for C60 solubilization from the ecotoxicological viewpoint.

## 4. Conclusions

The microstructuring of quercetin in polar organic solvent solutions is studied by using classical molecular dynamics simulations. These solutions are characterized by large heteroassociations through hydrogen bonding increasing with solvent polarity. The hydrogen bonding is developed through quercetin hydroxyl sites, being largely localized around several hydroxyl sites although remaining almost unaffected by the considered polar solvent. Nevertheless, these quercetin – organic solvent interactions are very dynamic, with hydrogen bonding living and reforming in a few picoseconds scale. The strong quercetin – organic solvent interactions provide changes in the polar organic solvent properties, which leads to different behavior when fullerene nanoparticles are dissolved in comparison with neat solvents. Therefore, C60 fullerene behavior is characterized by a largely heterogeneous solvation with solvent adopting a sandwich – like structure with alternating layers of organic solvent and quercetin, with the organic solvent in direct contact with the surface of the fullerene and flavonoid molecule being placed in a second external solvation

shell. Therefore, this nanoscopic arrangement allows an efficient fullerene solvation through interactions with the organic solvent and quercetin molecules, as well as maintaining the efficient quercetin – organic solvent hydrogen bonding. This study proposes the use of flavonoids as solubility enhancer for fullerenes in polar organic solvents.

### CRediT authorship contribution statement

**Juan Antonio Tamayo-Ramos:** Conceptualization, Methodology, Resources, Writing – original draft, Writing – review & editing, Supervision, Project administration, Funding acquisition. **Sonia Martel:** Conceptualization, Methodology, Writing – original draft, Writing – review & editing, Supervision, Project administration, Resources, Funding acquisition. **Rocío Barros:** Conceptualization, Methodology, Writing–original draft, Writing – review & editing, Supervision, Project administration, Resources, Funding acquisition. **Alfredo Bol:** Conceptualization, Methodology, Funding acquisition, Supervision, Project administration, Resources, Writing–original draft. **Mert Atilhan:** Conceptualization, Methodology, Supervision, Writing–original draft, Writing – review & editing. **Santiago Aparicio:** Conceptualization, Methodology, Resources, Writing–original draft, Writing – review & editing, Supervision, Project administration, Funding acquisition.

### Declaration of Competing Interest

The authors declare that they have no known competing financial interests or personal relationships that could have appeared to influence the work reported in this paper.

### Acknowledgements

This work was funded by Junta de Castilla y Leon (Spain, project NANOCOMP - BU058P20) and Ministerio de Ciencia, Innovación y Universidades (Spain, project RTI2018-101987-B-I00). We also acknowledge SCAYLE (Supercomputación Castilla y León, Spain) for providing supercomputing facilities. The statements made herein are solely the responsibility of the authors.

### Appendix A. Supplementary material

Supplementary data to this article can be found online at <https://doi.org/10.1016/j.molliq.2021.117714>.

### References

- [1] I.C.W. Arts, P.C.H. Hollman, Polyphenols and disease risk in epidemiologic studies, *Am. J. Clin. Nutr.* 81 (2005) 317s.
- [2] A.N. Panche, A.D. Diwan, S.R. Chandra, Flavonoids: an overview, *J. Nutr. Sci.* 5 (2016) e47.
- [3] G. Williamson, C.D. Kay, A. Crozier, The bioavailability, transport, and bioactivity of dietary flavonoids: a review from a historical perspective, *Comp. Rev. Food Sci. Food Saf.* 17 (5) (2018) 1054–1112.

- [4] T.K. Swetha, A. Priya, S.K. Pandian, in: *Plant Metabolites: Methods, Applications and Prospects*, Springer Singapore, Singapore, 2020, pp. 347–378, [https://doi.org/10.1007/978-981-15-5136-9\\_15](https://doi.org/10.1007/978-981-15-5136-9_15).
- [5] J.Oliveira-Chaves, M. Corre-de-Souza, I. Capelasso-da-Silva, D. Lachos-Perez, P. C. Torres-Mayanga, A.P. Fonseca-Machado, T. Forster-Carneiro, M. Vazquez-Espinosa, A. Velasco-Gonzalez, G. Fernandez-Barbero, M. Ariel-Rostagno, *Extraction of Flavonoids From Natural Sources Using Modern Techniques*, *Fron. Chem.* 8 (2020) 864.
- [6] M.L. Chavez-Gonzalez, L. Sepulveda, S.K. Verma, H.A. Luna-Garcia, L.V. Rodriguez-Duran, A. Iliina, C.N. Aguilar, *Conventional and Emerging Extraction Processes of Flavonoids*, *Processes* 8 (2020) 434.
- [7] Yuangang Zu, Weiwei Wu, Xiuhua Zhao, Yong Li, Weiguo Wang, Chen Zhong, Yin Zhang, Xue Zhao, *Enhancement of solubility, antioxidant ability and bioavailability of taxifolin nanoparticles by liquid antisolvent precipitation technique*, *Int. J. Pharm.* 471 (1–2) (2014) 366–376.
- [8] Magdalena Biesaga, *Influence of extraction methods on stability of flavonoids*, *J. Chromatogr. A* 1218 (18) (2011) 2505–2512.
- [9] M. Bianchi, R. Canavesi, S. Aprile, G. Grosa, E. Grosso, *Troloxerutin, a mixture of O-hydroxyethyl derivatives of the natural flavonoid rutin: Chemical stability and analytical aspects*, *J. Pharma. Biomed. Anal.* 150 (2018) 248–257.
- [10] T. Hattori, H. Tagawa, M. Inai, T. Kan, S.I. Kimura, S. Itai, S. Mitagotri, Y. Iwao, *Transdermal delivery of nobiletin using ionic liquids*, *Scientific Rep.* 9 (2019) 20191.
- [11] Daniella C Murador, Leonardo M de Souza Mesquita, Nicholas Vannuchi, Anna Rafaela C Braga, Veridiana V de Rosso, *Bioavailability and biological effects of bioactive compounds extracted with natural deep eutectic solvents and ionic liquids: advantages over conventional organic solvents*, *Curr. Opin. Food Sci.* 26 (2019) 25–34.
- [12] Juanjuan Zhao, Jun Yang, Yan Xie, *Improvement strategies for the oral bioavailability of poorly water-soluble flavonoids: An overview*, *Int. J. Pharma.* 570 (2019) 118642, <https://doi.org/10.1016/j.ijpharm.2019.118642>.
- [13] Shashank Kumar, Abhay K. Pandey, *Chemistry and biological activities of flavonoids: an overview*, *Scientific World J.* 2013 (2013) 1–16.
- [14] Enrico Finotti, D. Di Majo, *Influence of solvents on the antioxidant property of flavonoids*, *Nahrung.* 47 (3) (2003) 186–187.
- [15] Fernanda das Neves Costa, Gilda Guimarães Leitão, *Strategies of solvent system selection for the isolation of flavonoids by countercurrent chromatography*, *J. Sep. Sci.* 33 (3) (2010) 336–347.
- [16] Chao-Hui Feng, Juan Francisco García-Martín, María Broncano Lavado, María del Carmen López-Barrera, Paloma Álvarez-Mateos, *Evaluation of different solvents on flavonoids extraction efficiency from sweet oranges and ripe and immature Seville oranges*, *Int. J. Food Sci. Technol.* 55 (9) (2020) 3123–3134.
- [17] Maurice D. Awouafack, Pierre Tane, Hiroyuki Morita, in: *Flavonoids - From Biosynthesis to Human Health*, InTech, 2017, <https://doi.org/10.5772/67881>.
- [18] Huijie Zhang, Meng Wang, Lina Chen, Yanan Liu, Han Liu, Hongna Huo, Lili Sun, Xiaoliang Ren, Yanru Deng, Aidi Qi, *Structure-solubility relationships and thermodynamic aspects of solubility of some flavonoids in the solvents modeling biological media*, *J. Mol. Liq.* 225 (2017) 439–445.
- [19] Claudia Sandoval, Marcos Caroli Rezende, Fernando González-Nilo, *Solute-solvent interactions of flavonoids in organic solvents*, *J. Sol. Chem.* 32 (9) (2003) 781–790.
- [20] Manel Slimane, Mohamed Ghoul, Latifa Chebil, *Mesoscale modeling approach to study the dispersion and the solubility of flavonoids in organic solvents*, *Ind. Eng. Chem. Res.* 57 (37) (2018) 12519–12530.
- [21] Khadija Smail, Noureddine Tchour, Mohammed Barj, Bogdan Marekha, A. Idrissi, *Luteolin organic solvent interactions. A molecular dynamics simulation analysis*, *J. Mol. Liq.* 212 (2015) 503–508.
- [22] M. Jabbari, N. Khosravi, M. Feizabadi, D. Ajloo, *Solubility temperature and solvent dependence and preferential solvation of citrus flavonoid naringin in aqueous DMSO mixtures: an experimental and molecular dynamics simulation study*, *RSC Adv.* 7 (2017) 14776–14789.
- [23] H.F. Tooski, M. Jabbari, A. Farajtabar, *Solubility and preferential solvation of the flavonoid naringenin in some aqueous/organic solvent mixtures*, *J. Sol. Chem.* 45 (2016) 1701–1714.
- [24] S. Gupta, N. Basant, *Predictive modeling: Solubility of C60 and C70 fullerenes in diverse solvents*, *Chemosphere* 201 (2018) 361–369.
- [25] P. Cyswski, *Application of the Consonance solvent concept for accurate prediction of buckminster solubility in 180 net solvents using COSMO-RS Approach*, *Symmetry* 11 (2019) 828.
- [26] J.B. Ghasemi, M. Salahinejad, M.K. Rofouei, *Alignment independent 3D-QSAR modeling of fullerene (C60) solubility in different organic solvents*, *Fullerenes, Nanotubes and Carbon Nanostructures* 21 (2013) 367–380.
- [27] K.N. Semenov, N.A. Charykov, V.A., Keskinov, A.K. Piartman, A.A. Blokhin, A.A. Kopyrin, A.A.: *Solubility of light fullerenes in organic solvents*, *J. Chem. Eng. Data* 55 (2010) 13–36.
- [28] Nikolay O. Mchedlov-Petrosyan, *Fullerenes in molecular liquids. Solutions in "good" solvents: another view*, *J. Mol. Liq.* 161 (1) (2011) 1–12.
- [29] S. Goodarzi, T. Da Ros, J. Conde, F. Sefat, M. Mozafari, *Fullerene: biomedical engineers get to revisit an old friend*, *Materials Today* 20 (2017) 460–480.
- [30] V.S. Lata, *Modeling the Solubility of C70 fullerenes in diverse solvents: role of quantum-mechanical descriptors*, *Mol. Inf.* 38 (2019) 1800112.
- [31] V.C. Chaban, C. Maciel, E.E. Fileti, *Does the Like Dissolves Like Rule Hold for Fullerene and Ionic Liquids?*, *J. Sol. Chem.* 43 (2014) 1019–1031.
- [32] N.D. Oktaviyanti, K. Kartini, M.A. Hadiyat, E. Rachmawati, A.C. Wijaya, H. Hayun, A. Munim, *A green extraction design for enhancing flavonoid compounds from Ixora javanica flowers using a deep eutectic solvent*, *R. Soc. Open Sci.* 7 (2020) 201116.
- [33] Latifa Chebil, Catherine Humeau, Julie Anthoni, François Dehez, Jean-Marc Engasser, Mohamed Ghoul, *Solubility of flavonoids in organic solvents*, *J. Chem. Eng. Data* 52 (5) (2007) 1552–1556.
- [34] Y. Zhang, N. Wang, L. Zou, M. Zhang, R. Chi, *Molecular dynamics simulation on the dissolution process of Kaempferol cluster*, *J. Mo. Liq.* 304 (2020) 112779.
- [35] Zhen Cao, Yuxing Peng, Shu Li, Lei Liu, Tianying Yan, *Molecular dynamics simulation of fullerene C60 in ethanol solution*, *J. Phys. Chem. C* 113 (8) (2009) 3096–3104.
- [36] Gregorio García, Mert Atilhan, Santiago Aparicio, *Theoretical study on the solvation of C60 fullerene by ionic liquids*, *J. Phys. Chem. B* 118 (38) (2014) 11330–11340.
- [37] James S. Peerless, G. Hunter Bowers, Albert L. Kwansa, Yaroslava G. Yingling, *Effect of C60 adducts on the dynamic structure of aromatic solvation shells*, *Chem. Phys. Lett.* 678 (2017) 79–84.
- [38] S. Singh, *Dynamics of the mixtures of fullerene-60 and aromatic solvents: A molecular dynamics approach*, *J. Phys. Org. Chem.* 33 (2020) e4103.
- [39] Kazeem O. Sulaiman, Abdulmujeeb T. Onawole, Omar Faye, Damola T. Shuaib, *Understanding the corrosion inhibition of mild steel by selected green compounds using chemical quantum based assessments and molecular dynamics simulations*, *J. Mol. Liq.* 279 (2019) 342–350.
- [40] A. P. Lyubartsev, A. Laaksonen, M.DynaMix – a scalable portable parallel MD simulation package for arbitrary molecular mixtures. *Comput. Phys. Commun.* 2000, 128, 565–589.
- [41] L. Martínez, R. rade, E. G. Birgin, J. M. Martínez, *PACKMOL: a package for building initial configurations for molecular dynamics simulations*, *J. Comput. Chem.* 2009, 30, 2157–2164.
- [42] V. Zoete, M.A. Cuendet, A. Grossdidier, O. Michielin, *SwissParam, a fast force field generation tool for small organic molecules*, *J. Comput. Chem.* 32 (2011) 2359–2368.
- [43] M. Tuckerman, B.J. Berne, G.J. Martyna, *Reversible multiple time scale molecular dynamics*, *J. Chem. Phys.* 97 (1992) 1990–2001.
- [44] U.L. Essmann, M.L. Perera, T. Berkowitz, H. Darden, H. Lee, L.G. Pedersen, *A smooth particle mesh Ewald method*, *J. Chem. Phys.* 103 (3) (1995) 8577–8593.
- [45] M. Brehm, B. Kirchner, *TRAVIS - A free analyzer and visualizer for Monte Carlo and Molecular Dynamics trajectories*, *J. Chem. Inf. Model.* 51 (2011) 2007–2023.
- [46] W. Humphrey, A. Dalke, K. Schulten, *VMD - Visual molecular dynamics*, *J. Molec. Graphics* 14 (1996) 33–38.
- [47] Karin Aschberger, Helinor J. Johnston, Vicki Stone, Robert J. Aitken, C. Lang Tran, Steven M. Hankin, Sheona A.K. Peters, Frans M. Christensen, *Review of fullerene toxicity and exposure – Appraisal of a human health risk assessment, based on open literature*, *Regul. Toxicol. Pharmacol.* 58 (3) (2010) 455–473.
- [48] H. Yang, C. Lou, L. Sun, J. Li, Y. Cai, Z. Wang, W. Li, G. Liu, Y. Tang, *AdmetSAR 2.0: web-service for prediction and optimization of chemical ADMET properties*, *Bioinformatics* 35 (2019) 1067–1069.
- [49] N.F. Lago, M. Alberti, A. Lombardi, f. Pirani, *A force field for acetone: the transition from small clusters to liquid phase investigated by molecular dynamics simulations*, *Theor.Cehm. Acc.* 135 (2016) 161.
- [50] Aleksey Vishnyakov, Alexander P. Lyubartsev, Aatto Laaksonen, *Molecular dynamics simulations of dimethyl sulfoxide and dimethyl sulfoxide–water mixture*, *J. Phys. Chem. A* 105 (10) (2001) 1702–1710.
- [51] Yi Lei, Haoran Li, Haihua Pan, Shijun Han, *Structures and hydrogen bonding analysis of n, n-dimethylformamide and N, N-dimethylformamide-water mixtures by molecular dynamics simulations*, *J. Phys. Chem. A* 107 (10) (2003) 1574–1583.
- [52] M. Brehm, M. Thomas, S. Gehrke, B. Kirchner, *TRAVIS—A free analyzer for trajectories from molecular simulation*, *J. Chem. Phys.* 152 (2020) 164105.
- [53] M.D. Mohammadi, M. Hamzehloo, *Densities, viscosities, and refractive indices of binary and ternary mixtures of methanol, acetone, and chloroform at temperatures from (298.15–318.15) K and ambient pressure*, *Fluid Phase Equilib.* 483 (2019) 14–30.
- [54] Xiaojuan Chen, Zhaoxun Lian, Haimin Zhong, Liuping Chen, *Intradiffusion, density and viscosity studies in binary liquid systems of acetylacetone + DMF/DMSO/benzene at 303.15 K and 333.15 K*, *Chin. J. Chem. Eng.* 23 (10) (2015) 1679–1684.
- [55] Vitaly V. Chaban, Cleiton Maciel, Eudes Eterno Fileti, *Solvent polarity considerations are unable to describe fullerene solvation behavior*, *J. Phys. Chem. B* 118 (12) (2014) 3378–3384.
- [56] Loukia Maritsa, Sonia Martel, Rocío Barros, Alfredo Bol, Santiago Aparicio, *Addition of MoS<sub>2</sub> nanosheets to synthetic poly-alpha-olefins base oils: A theoretical study of nanolubrication*, *J. Mol. Liq.* 332 (2021) 115881, <https://doi.org/10.1016/j.molliq.2021.115881>.
- [57] L. Maritsa, A. Bol, S. Aparicio, *Quasi-smectic liquid crystal phase of octane in contact with 2D MoS<sub>2</sub>*, *Appl. Surf. Sci.* 533 (2020) 147386.
- [58] L. Maritsa, A. Bol, S. Aparicio, *Densification and tribofilm formation in hydrocarbon nanofluids induced by MoS<sub>2</sub> nanotubes*, *J. Mol. Liq.* 311 (2020) 113291.
- [59] M. Baldrighi, M. Trusel, R. Tonini, S. Giordani, *Carbon Nanomaterials Interfacing with Neurons: An In vivo Perspective*, *Front. Neurosci.* 10 (2016) 250.